Design and Preparation of Supported Au Catalyst with Enhanced Catalytic Activities by Rationally Positioning Au Nanoparticles on Anatase

ARTICLE *in* JOURNAL OF PHYSICAL CHEMISTRY LETTERS · JUNE 2015

Impact Factor: 7.46 · DOI: 10.1021/acs.jpclett.5b00655

THE JOURNAL OF PHYSICAL CHEMISTRY Letters

Letter

pubs.acs.org/JPCL

Design and Preparation of Supported Au Catalyst with Enhanced Catalytic Activities by Rationally Positioning Au Nanoparticles on Anatase

Liang Wang,[‡] Hong Wang,*[,†] Andrew E. Rice,[†] Wei Zhang,*[,§] Xiaokun Li,[∥] Mingshu Chen,[∥] Xiangju Meng,[‡] James P. Lewis,[†] and Feng-Shou Xiao*[,‡]

[†]Department of Physics and Astronomy, West Virginia University, 135 Willey Street, Morgantown, West Virginia 26506-6315, United States

[‡]Key Lab of Applied Chemistry of Zhejiang Province, Department of Chemistry, Zhejiang University, Hangzhou 310028, P. R. China

[§]Department of Materials Science and Key Laboratory of Mobile Materials MOE, Jilin University, Changchun 130012, P. R. China

[∥]State Key Laboratory of Physical Chemistry of Solid Surfaces, National Engineering Laboratory for Green Chemical Productions of Alcohols-Ethers-Esters, Xiamen University, Xiamen 361005, P. R. China

Supporting Information

ABSTRACT: A synergistic effect between individual components is crucial for increasing the activity of metal/metal oxide catalysts. The greatest challenge is how to control the synergistic effect to obtain enhanced catalytic performance. Through density functional theory calculations of model Au/TiO_2 catalysts, it is suggested that there is strong interaction between Au nanoparticles and Ti species at the edge/corner sites of anatase, which is favorable for the formation of stable oxygen vacancies. Motivated by this theoretical analysis, we have rationally prepared Au nanoparticles attached to edge/corner sites of anatase support (Au/TiO_2-EC), confirmed by their HR-TEM images. As expected, this strong interaction is well characterized by Raman, UV−visible, and XPS techniques. Very interestingly, compared with conventional Au catalysts, Au/TiO_2-EC exhibits superior catalytic activity in the oxidations using O_2. Our approach to controlling Au nanoparticle positioning on anatase to obtain enhanced catalytic activity offers an efficient strategy for developing more novel supported metal catalysts.

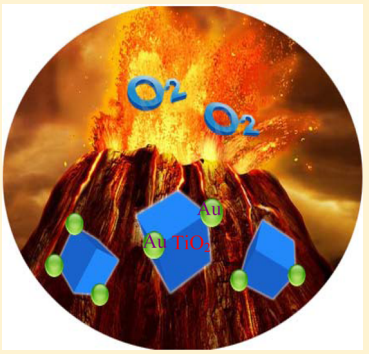

Synergy serves as the engine driving the individual components in cooperation to enhance catalytic activity or selectivity. In particular, for the oxide-supported Au nanocatalysts, significantly increased activity has been observed once the two components are conjoined, even though each component is relatively inert.[1−3] Extensive studies have attempted to generalize the "synergy" mechanism of heterogeneous catalysts,[4,5] but few successfully grasp the nature of this "magic" cooperation in terms of the role of oxide supports. TiO_2 has been studied as one of the most applicable oxide supports, and some reports suggest that the electronic interactions between Au and TiO_2 contribute substantially in strengthening the catalytic activity.[6−10] Even though significant progress has been achieved for Au/TiO_2 catalyst, it is still a significant challenge to understand the microscopic mechanisms regarding the catalytic activity. The key criteria is to synthesize novel catalysts by rationally controlling the synergistic effect.

Here we design a catalyst to enhance the complex features of nanostructural Au/TiO_2. When brought into intimate contact, the positioning of the Au nanoparticles on the anatase nanostructures strongly determines the resulting nature of their interaction. Interestingly, it turns out that Au nanoparticles attached to the edge/corner sites of anatase cooperate with the Ti species, forming potential oxygen vacancies near the attaching region. Motivated by our initial computational observations, we rationally synthesized a nanostructural anatase supported Au nanoparticles (labeled Au/TiO_2-EC throughout), whose distinguishing feature is the formation of oxygen vacancies by increased proportion of Au nanoparticles attached to edge/corner sites on anatase support. Remarkably, Au/TiO_2-EC exhibits superior catalytic activities in the oxidations of styrene and CO.

Applying density functional theory in our computational investigation,[11] we have built an anatase nanostructure emphasizing the connection between (001) and (101) facets.

By creating anatase nanostructure (308 atoms, TiO_2-308, Figure S1a in the SI) in this manner, we obtain several low-coordinated Ti sites also referred to as corner/edge sites, which serve as "hot" adsorption spots. Considering all of the possible attaching sites, we attached Au_{13}, a representative of gold nanoparticles, to several locations, including the facet sites on (001) or (101) surfaces, and the edged sites (Figures S1−S3 in

Received: March 30, 2015
Accepted: June 4, 2015

DOI: 10.1021/acs.jpclett.5b00655
J. Phys. Chem. Lett. 2015, 6, 2345−2349

the SI). After full optimization, the edge site adjoining the (101) facet has the lowest adsorption energy. The relaxed structure exhibits unexpected structural changes, in particular, the region around the Au_{13} nanoparticle. Checking the distance between the Au and Ti atoms (ranging between 2.62 and 2.72 Å), we have found that there is a strong interaction between Au and Ti atoms (Figure 1A). Meanwhile, oxygen atoms are

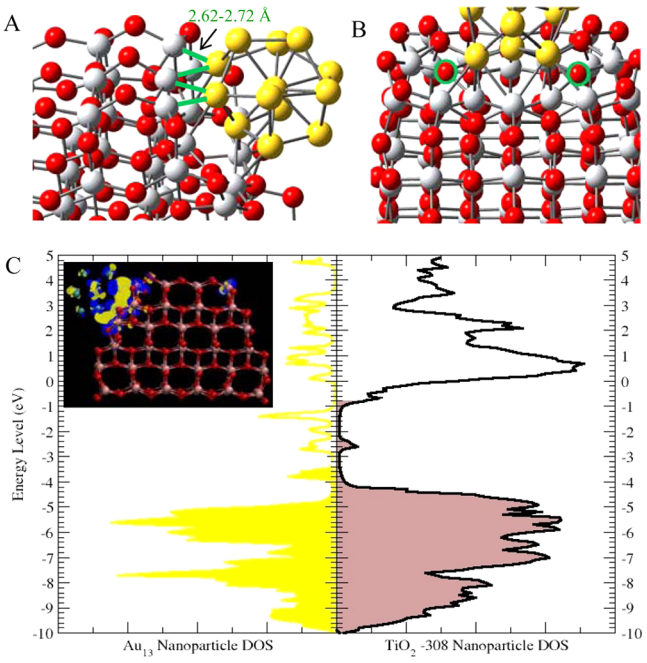

Figure 1. (A,B) Zoom-in images of the optimized Au_{13}/TiO_2-308 structure. The green circles in panel B label the oxygen atoms, which turn out to be the possible oxygen vacancies. (C) Yellow plot is the density of states (DOS) of Au_{13} with both filled and empty states labeled. The black plot is the DOS of TiO_2-308 anatase. The area filled with light-brown color represents filled states. (Insert image in panel C is the charge density difference of the Au_{13}/TiO_2-308 structure. The contour value is 0.03.)

pushed away by this strong interaction between Ti and Au atoms (Figure 1B). More importantly, there are five Au atoms of the Au_{13} nanoparticle that interact with Ti atoms strongly, which potentially creates oxygen vacancies in the attached region. (See discussion in Figure S3 in the SI.) In particular, two of the Au atoms form a zip line with the edged Ti atoms. On the basis of the optimized structure, we confirm that all three edged Ti atoms interact strongly with Au atoms (Figure 1A). As a result, the edged Ti atoms function importantly to interact with the Au_{13} nanoparticle (Figure 1). In contrast, we did not observe any surface oxygen atoms moving away after Au_{13} attaches to the anatase (101) surface (Figure S4 in the SI).

By analyzing the electronic properties, we expect to understand the interactions from principle. The charge density difference is constructed by subtracting the total election density of Au_{13}/TiO_2-308 from the density of Au_{13} and TiO_2-308 without modifying the atomic positions. As shown in Figure 1C, there is significant charge density difference that increases between Au and Ti atoms. The increased density is closer to the Au atoms, indicating that the charge transfer occurs from Ti to Au. The low-coordinated Ti atoms exhibit localized electronic states with unpaired electrons at roughly −2.8 eV, (Figure 1C), which is very close in energy to the LUMO of Au_{13}. This energy alignment resulted in a strong coupling between the filled Ti states and the empty states of Au_{13}, thus promoting the charge transfer from Ti atom to Au atom. On the basis of this evidence, we hypothesize that the intimate interaction between the Au atoms and the edged/cornered Ti atoms possibly creates oxygen vacancies between these Au and Ti species. On the basis of our results, the oxygen vacancies possibly originate at the site where the oxygen atoms are pushed away by the Au attachment (Figures S5 and S6 in the SI). Therefore, small Au nanoparticles interact with nanostructural TiO_2 in a very strong manner and induce oxygen vacancies forming at the interface.

According to these theoretical analyses, we expect to prepare supported Au nanoparticles with extraordinarily high catalytic activities by rationally controlling the position of Au nanoparticles on the edge/corner of TiO_2 support. Herein, we successfully fabricated Au nanoparticles selectively attached on the edge/corner of nano-anatase (30−40 nm) by employing polyvinylpyrrolidone ligand. After removing the ligand by calcination, Au/TiO_2-EC was obtained. In comparison, conventional deposition−precipitation of anatase-supported Au nanoparticles is also prepared (Au/TiO_2-Con). Both samples have the same anatase support, very similar Au loadings (0.87−0.91 wt %), particle size distributions (see details in Figures S7−S10 in the SI), and Au dispersion degree (19.9−21.5%, Table S1 in the SI), but they have quite distinguishable catalytic activities in oxidations of styrene and CO with molecular oxygen.

Figure 2 shows HR-TEM images of the random selected areas of Au/TiO_2-Con and Au/TiO_2-EC samples. For Au/TiO_2-Con, most of the Au nanoparticles are found on the (101) surface of anatase (Figure 2a−c), which is the primary surface of nanostructural anatase. By analyzing more than 100 Au nanoparticles randomly selected, we confirm that 86% of the Au nanoparticles of Au/TiO_2-Con sample are located on the (101) surface of anatase. Distinctively, the Au nanoparticles of the Au/TiO_2-EC sample preferentially locate on the edge/corner sites of anatase (Figure 2d−f and Figure S11 in the SI), where no specific anatase planes could be found to interact with gold nanoparticles. (The percentage of Au nanoparticles on edge/corner sites was estimated to be >75%.) The distinct features of Au/TiO_2-EC are strongly correlated to the key role of the PVP ligand, which serves to protect and maintain higher stability of the Au nanoparticles compared with the deposition−precipitation method (without PVP). The former facilitates Au nanoparticles to anchor at the edge/corner sites, which are energetically favorable sites for Au-anatase system (Figure S3 in the SI).

Thus, it comes to the grand question: Does the attaching site for Au nanoparticles on anatase lead to the formation of oxygen vacancies as we predict in the computational models? Figure S12 in the SI shows the Raman spectra of various samples. Au/TiO_2-Con presents two Raman modes of E_g at 146 and 198 cm^{-1}, which are similar to the E_g modes of anatase at 143 and 197 cm^{-1}. The Au/TiO_2-EC sample also exhibits the Raman modes of E_g at 154 and 205 cm^{-1}, which are shifted by 11 and 8 cm^{-1} from those of anatase, respectively. In consideration of the fact that the sole oxygen vacancy on TiO_2 can only cause new weak modes at wave numbers higher than 300 cm^{-1} in the literature,[12,13] the shift of Raman modes on Au/TiO_2-EC is indicatively related to the strong interaction between Au and Ti during the formation of oxygen vacancy on Au/TiO_2-EC, which would change the symmetry of Ti−O−Ti species around the Au nanoparticles.[12,13] In the Au 4f XPS spectra (Figure S13A in

DOI: 10.1021/acs.jpclett.5b00655
J. Phys. Chem. Lett. 2015, 6, 2345−2349

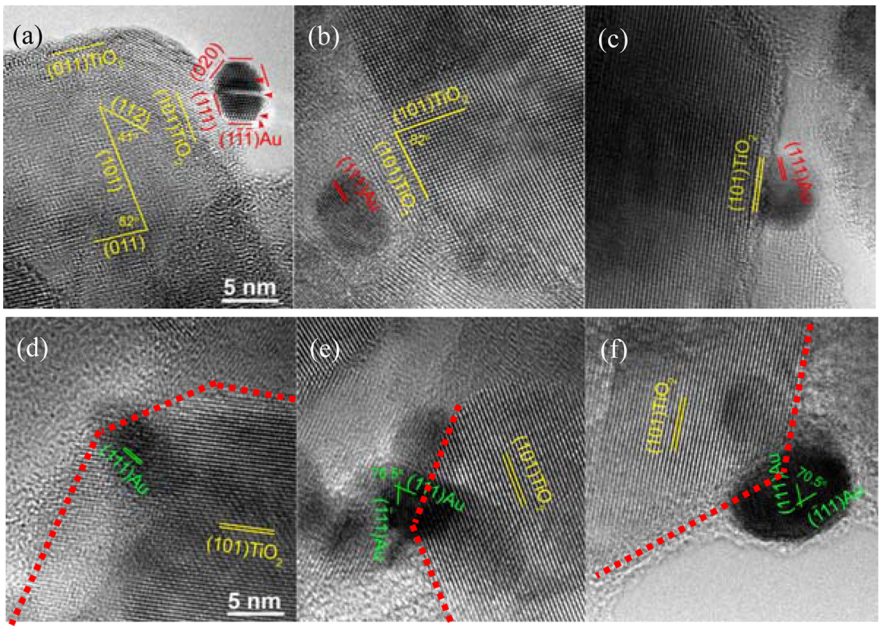

Figure 2. HR-TEM images of the random selected areas of (a–c) Au/TiO_2-Con and (d–f) Au/TiO_2-EC samples. The red lines represent the surfaces of nanosized anatase.

the SI), the Au/TiO_2-EC sample that exhibits the binding energy of Au $4f_{7/2}$ is at 83.1 eV (0.9 eV shift from that of typical metallic Au^0 84.0 eV), which indicates the Au nanoparticles on Au/TiO_2-EC are negatively charged compared with Au.[14] In contrast, the Au/TiO_2-Con sample shows that Au $4f_{7/2}$ binding energy is ~83.8 eV, similar to 84.0 eV of metallic Au^0. Furthermore, the Ti 2p XPS spectra of anatase and Au/TiO_2-Con exhibit Ti $2p_{3/2}$ peak at 458.8 eV (Figure S13B in the SI), assigning to typical Ti^{4+} species.[15] Interestingly, the Ti $2p_{3/2}$ spectrum of Au/TiO_2-EC shows additional peaks at 458.4 and 457.8 eV. All of these results demonstrate the Ti species of anatase and Au/TiO_2-Con exhibit similar electronic properties, which are quite different from those of Au/TiO_2-EC sample (Figure S13B in the SI). For the Au/TiO_2-EC sample, it is proposed that the oxygen vacancy transfers the extra electrons to the adjacent Ti and Au atoms (Figure 1c), forming the strong electronic interaction between Au and Ti, which is in excellent agreement with the results from computational models (Figure 1).[16]

We study the catalytic properties of Au catalysts by employing the oxidation of styrene at first, which has been widely investigated over various Au catalysts.[17−19] In the aerobic oxidation of styrene, molecular oxygen activation has been considered as the initial step over Au nanoparticle catalysts for this reaction in the absence of any initiator. In general, the ultrasmall Au nanoclusters (~1.4 nm) have been used as efficient catalysts for the aerobic oxidation styrene oxidation by molecular oxygen.[18,19] Table 1 presents the catalytic data of various catalysts in the oxidation of styrene by molecular oxygen. As presented in Table 1, pure anatase is completely inactive for the reaction (entry 1). However, the Au/TiO_2-EC catalyst exhibited very high styrene conversion at 56.0%, with selectivity to styrene epoxide at 17.5% (entry 2). In contrast, the Au/TiO_2-Con catalyst presents relatively low conversion of styrene at 29.2% with selectivity to styrene epoxide at 10.4% (entry 3). As we previously analyzed, the Au/TiO_2-EC and the Au/TiO_2-Con samples share the same anatase supports, similar Au content, nanoparticle size distribution, and Au dispersion degree. Therefore, the high activity of the Au/TiO_2-EC is directly related to the formation of oxygen vacancy by the interactions between Au and Ti, which could boost their catalytic activity to molecular oxygen (Figures S14 and S15 in the SI). Furthermore, by decreasing the oxygen pressure to 1.5 bar, we confirm that the Au/TiO_2-EC catalyst still exhibits higher styrene conversion at 41.5%, much higher than that (20%) of the Au/TiO_2-Con (entries 4 and 5). The Au nanoclusters (~1.4 nm) supported on boron nitride (Au_{55}/BN) and SiO_2 (Au_{55}/SiO_2, Figure S16 in the SI) (both reported as efficient catalysts for the aerobic oxidation of styrene) show styrene conversion at 19.2–25.8%, with styrene

Table 1. Catalytic Data of Various Au Catalysts in Oxidation of Styrene by Molecular Oxygen[a]

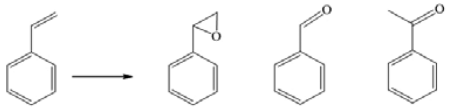

			product selectivity (%)[b]			
entry	catalyst	conv. (%)	P1	P2	P3	P4
1	anatase					
2	Au/TiO_2-EC	56.0	17.5	70.0	4.5	8.0
3	Au/TiO_2-Con	29.2	10.4	82.6	2.0	5.0
4[c]	Au/TiO_2-EC	41.5	11.0	75.3	6.3	7.4
5[c]	Au/TiO_2-Con	20.0	8.8	79.2	4.5	7.5
6[c,d]	Au_{55}/BN	19.2	14.0	82.3	3.9	
7[c,d]	Au_{55}/SiO_2	25.8	12.0	82.1	5.7	
8[c]	Au_{55}/SiO_2[e]	24.3	13.7	80.6	4.9	0.8

[a]Reaction conditions: 100 mg of catalyst, 12 mmol of styrene, 20 mL of toluene, 10.0 bar of O_2, 100 °C, 15 h, dodecane as internal standard. The standard deviation of styrene conversion and product selectivity is <2%. [b]P1 = styrene epoxide, P2 = benzaldehyde, P3 = acetophenone, P4 = phenylacetaldehyde, benzyl alcohol, and others. [c]1.5 bar of O_2. [d]Data are from ref 19. [e]Au_{55}/SiO_2 catalyst is synthesized and the catalytic tests are performed according to the methods in ref 19.

DOI: 10.1021/acs.jpclett.5b00655
J. Phys. Chem. Lett. 2015, 6, 2345−2349

epoxide selectivity at 12−14% (entries 6−8).[22] Additionally, further study (Figure S17 and Table S2 in the SI) demonstrates that the reaction over Au/TiO_2-EC is faster (58.2 mmol L^{-1} h^{-1}) than those over Au/TiO_2-Con (29.4 mmol L^{-1} h^{-1}) and Au_{55}/SiO_2 (36.0 mmol L^{-1} h^{-1}). Furthermore, it is worth noting that the turnover frequency (TOF) of Au/TiO_2-EC could reach as high as 174.6 h^{-1}, higher than that over Au_{55}/SiO_2 (108.0 h^{-1}). These results indicate the superior catalytic activity of Au/TiO_2-EC in styrene oxidation. Moreover, we find that the Au/TiO_2-EC exhibits excellent stability and recyclability during the whole process (Figure 3). After recycling for six times in the styrene oxidation, the Au/TiO_2-EC sample still has unchanged Au particle size and strong Au−Ti interaction, indicating the high stability of Au nanoparticles on the edge/corner sites of nano-anatase support (Figures S18−S20 in the SI). On the contrary, the Au_{55} clusters obviously lose the activity after two further cycles under the same reaction conditions because of the aggregation of Au_{55} clusters into relatively large nanoparticles during the reaction process (Figure S21in the SI).[19]

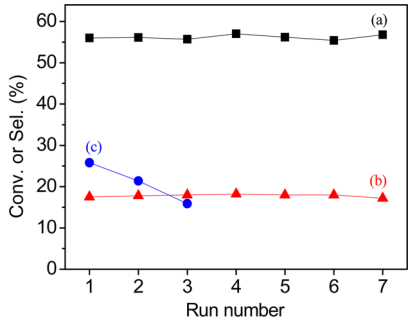

Figure 3. Aerobic oxidation of styrene using Au/TiO_2-EC and Au_{55}/SiO_2 catalysts over several cycles. (a) Styrene conversion over Au/TiO_2-EC, (b) epoxide selectivity over Au/TiO_2-EC, and (c) styrene conversion over Au_{55}/SiO_2. The data for the Au_{55}/SiO_2 catalyst are from ref 19.

Additionally, we have also studied the catalytic activities of Au/TiO_2-EC and Au/TiO_2-Con in a widely investigated model reaction of CO oxidation,[20−23] a reaction that is sensitive to the presence of oxygen vacancies.[20] As shown in Figure 4, Au/TiO_2-EC yields full conversion of CO at 168 °C. In contrast, even at high temperature of 272 °C, the Au/TiO_2-Con catalyst still yields relatively low CO conversion at 56.8%. These results indicate that Au/TiO_2-EC exhibits much higher activity in CO oxidation as compared with Au/TiO_2-Con, which is attributed to the formation of oxygen vacancies by the stable electronic interaction between Au and Ti atoms in Au/TiO_2-EC.

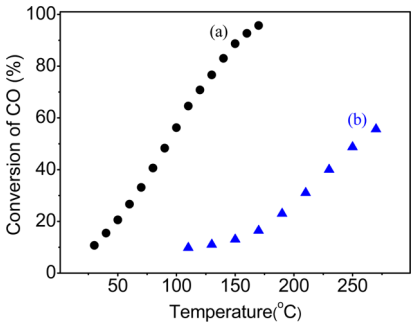

Figure 4. Catalytic oxidation of CO over (a) Au/TiO_2-EC and (b) Au/TiO_2-Con catalysts.

In summary, we have developed an efficient way to boost the activity of Au nanocatalysts. Coupling computational models with synthesis and characterization, the cooperation between Au and anatase is significantly enhanced by rationally positioning the Au nanoparticles on the edged/corner sites. The strong interaction between Au and the Ti species around the edge/corner sites promotes oxygen vacancies that enhance catalytic activity. More importantly, the Au/TiO_2-EC exhibits high catalytic activity and excellent recyclability in the oxidation of styrene and CO. Our investigation on the interaction of Au nanoparticles positioned on the edge/corner sites of TiO_2 supports offers an excellent opportunity for designing and developing highly "controlled" catalysts in the future.

■ ASSOCIATED CONTENT

Ⓢ Supporting Information

Experimental and computational details and characterizations including XPS, UV−vis, Raman, TEM, and O_2-TPD. The Supporting Information is available free of charge on the ACS Publications website at DOI: 10.1021/acs.jpclett.5b00655.

■ AUTHOR INFORMATION

Corresponding Authors

*E-mail: hong.wang@mail.wvu.edu (H.W.)
*E-mail: weizhang@jlu.edu.cn (W.Z.)
*E-mail: fsxiao@zju.edu.cn (F.-S.X.).

Notes

The authors declare no competing financial interest.

■ ACKNOWLEDGMENTS

This work is supported by National Science Foundation (DMREF CHE-1434378), Department of Energy (DE-SC0004737), National Natural Science Foundation of China (21333009, U146220026, and 21403192), National High-Tech Research and Development Program of China (2013AA065301), and Special Funding for Academic Leaders in Jilin University (No. 419080500273).

■ REFERENCES

(1) Gates, B. C. Supported Metal Clusters: Synthesis, Structure, and Catalysis. *Chem. Rev.* **1995**, *95*, 511−522.
(2) Corma, A.; Garcia, H. Supported Gold Nanoparticles as Catalysts for Organic Reactions. *Chem. Soc. Rev.* **2008**, *37*, 2096−2126.
(3) Hayashi, T.; Tanaka, K.; Haruta, M. Selective Vapor-Phase Epoxidation of Propylene over Au/TiO_2 Catalysts in the Presence of Oxygen and Hydrogen. *J. Catal.* **1998**, *178*, 566−575.
(4) Haruta, M.; Date, M. Advances in the Catalysis of Au Nanoparticles. *Appl. Catal., A* **2001**, *222*, 427−437.
(5) Min, B. K.; Friend, C. M. Heterogeneous Gold-Based Catalysis for Green Chemistry: Low-Temperature CO Oxidation and Propene Oxidation. *Chem. Rev.* **2007**, *107*, 2709−2724.
(6) Liu, X.; He, L.; Liu, Y. M.; Cao, Y. Supported Gold Catalysis: From Small Molecule Activation to Green Chemical Synthesis. *Acc. Chem. Res.* **2014**, *47*, 793−804.
(7) Shen, Y.; Zhang, S.; Li, H.; Ren, Y.; Liu, H. C. Efficient Synthesis of Lactic Acid by Aerobic Oxidation of Glycerol on Au-Pt/TiO_2 Catalysts. *Chem.—Eur. J.* **2010**, *16*, 7368−7371.
(8) Pan, M.; Brush, A. J.; Dong, G.; Mullins, C. B. Tunable Ether Production via Coupling of Aldehydes or Aldehyde/Alcohol over Hydrogen-Modified Gold Catalysts at Low Temperatures. *J. Phys. Chem. Lett.* **2012**, *3*, 2512−2516.

DOI: 10.1021/acs.jpclett.5b00655
J. Phys. Chem. Lett. 2015, 6, 2345−2349

(9) Xing, M.-Y.; Yang, B.-B.; Yu, H.; Tian, B.-Z.; Bagwasi, S.; Zhang, J.-L.; Gong, X.-Q. Enhanced Photocatalysis by Au Nanoparticle Loading on TiO_2 Single-Crystal (001) and (110) Facets. *J. Phys. Chem. Lett.* **2013**, *4*, 3910−3917.
(10) Baranovskii, S. D.; Wiemer, M.; Nenashev, A. V.; Jansson, F.; Gebhard, F. Calculating the Efficiency of Exciton Dissociation at the Interface between a Conjugated Polymer and an Electron Acceptor. *J. Phys. Chem. Lett.* **2012**, *3*, 1214−1221.
(11) Lewis, J. P.; Jelínek, P.; Ortega, J.; Demkov, A. A.; Trabada, D. G.; Haycock, B.; Wang, H.; Adams, G.; Tomfohr, J. K.; Abad, E.; Wang, H.; Drabold, D. A. Advances and Applications in the FIREBALL ab initio Tight-binding Molecular-Dynamics Formalism. *Phys. Status Solidi* **2011**, *248*, 1989−2007.
(12) Liu, G.; Li, F.; Wang, D. W.; Tang, D. M.; Liu, C.; Ma, X. L.; Lu, G. Q.; Cheng, H. M. Electron Field Emission of a Nitrogen-Doped TiO_2 Nanotube Array. *Nanotechnology* **2008**, *19*, 025606.
(13) Liu, G.; Yang, H. G.; Wang, X.; Cheng, L.; Lu, H.; Wang, L.; Lu, G. Q.; Cheng, H. M. Enhanced Photoactivity of Oxygen-Deficient Anatase TiO_2 Sheets with Dominant {001} Facets. *J. Phys. Chem. C* **2009**, *113*, 21784−21788.
(14) Si, R.; Flytzani-Stephanopoulos, M. Shape and Crystal-Plane Effects of Nanoscale Ceria on the Activity of Au-CeO_2 Catalysts for the Water-Gas Shift Reaction. *Angew. Chem., Int. Ed.* **2008**, *47*, 2884−2887.
(15) Zou, X.; Liu, J.; Su, J.; Zuo, F.; Chen, J.; Feng, P. Facile Synthesis of Thermal- and Photostable Titania with Paramagnetic Oxygen Vacancies for Visible-Light Photocatalysis. *Chem.—Eur. J.* **2013**, *19*, 2866−2873.
(16) Batzill, M.; Morales, E. H.; Diebold, U. Surface Studies of Nitrogen Implanted TiO_2. *Chem. Phys.* **2007**, *339*, 36−43.
(17) Hughes, M. D.; Xu, Y.; Jenkins, P.; McMorn, P.; Landon, P.; Enache, D. I.; Carley, A. F.; Attard, G. A.; Hutchings, G. J.; King, F.; Stitt, E. H.; Johnston, P.; Grifffin, K.; Kiely, C. J. Tunable Gold Catalysts for Selective Hydrocarbon Oxidation under Mild Conditions. *Nature* **2005**, *437*, 1132−1135.
(18) Liu, Y. M.; Tsunoyama, H.; Akita, T.; Tsukuda, T. Efficient and Selective Epoxidation of Styrene with TBHP Catalyzed by Au_{25} Clusters on Hydroxyapatite. *Chem. Commun.* **2010**, *46*, 550−552.
(19) Turner, M.; Golovko, V. B.; Vaughan, O. P. H.; Abdulkin, P.; Berenguer-Murcia, A.; Tikhov, M. S.; Johnson, B. F. G.; Lambert, R. M. Selective Oxidation with Dioxygen by Gold Nanoparticle Catalysts Derived from 55-atom Clusters. *Nature* **2008**, *454*, 981−983.
(20) Widmann, D.; Behm, R. J. Activation of Molecular Oxygen and the Nature of the Active Oxygen Species for CO Oxidation on Oxide Supported Au Catalysts. *Acc. Chem. Res.* **2014**, *47*, 740−749.
(21) Guzman, J.; Gates, B. C. Catalysis by Supported Gold: Correlation between Catalytic Activity for CO Oxidation and Oxidation States of Gold. *J. Am. Chem. Soc.* **2004**, *126*, 2672−2673.
(22) Yan, W. F.; Brown, S.; Pan, Z. W.; Mahurin, S. M.; Overbury, S. H.; Dai, S. Ultrastable Gold Nanocatalyst Supported by Nanosized Non-oxide Substrate. *Angew. Chem., Int. Ed.* **2006**, *45*, 3614−3618.
(23) Lin, C.; Liu, X.; Wu, S.-H.; Liu, K.-H.; Mou, C.-Y. Corking and Uncorking a Catalytic Yolk-Shell Nanoreactor: Stable Gold Catalyst in Hollow Silica Nanosphere. *J. Phys. Chem. Lett.* **2011**, *2*, 2984−2988.

DOI: 10.1021/acs.jpclett.5b00655
J. Phys. Chem. Lett. 2015, 6, 2345−2349